Characterization and integrated modelling of core radiative collapse in WEST plasmas

Valeria Ostuni, Jean François Artaud, Clarisse Bourdelle, Jorge Morales, Pierre Manas, Yves Peysson, Nicolas Fedorczak, Rémi Dumont, Marc Goniche, Patrick Maget

Characterization and integrated modelling of core radiative collapse in WEST plasmas

DE LA RECHERCHE À L'INDUSTRIE

US-EU Joint Transport Task Force 07/04/2022

V. Ostuni, J. Morales, J-F Artaud, C. Bourdelle, P. Manas, Y. Peysson, N. Fedorczak, R. Dumont, M. Goniche, P. Maget & WEST team

Outline

- Context;
- **Characterize** and **understand** the dynamics of the **radiative collapse** observed in WEST operation;
- **Reproduce** the rapid **collapse** of **central temperature** using an integrated model framework to **understand** which are the **actuators** that lead to the observed dynamics;
- Conclusions.

Outline

- **Context;**
- Characterize and understand the dynamics of the radiative collapse observed in WEST operation;
- Reproduce the rapid collapse of central temperature using an integrated model framework to understand which are the actuators that lead to the observed dynamics;
- Conclusions.

WEST: superconducting full W environment heated by RF

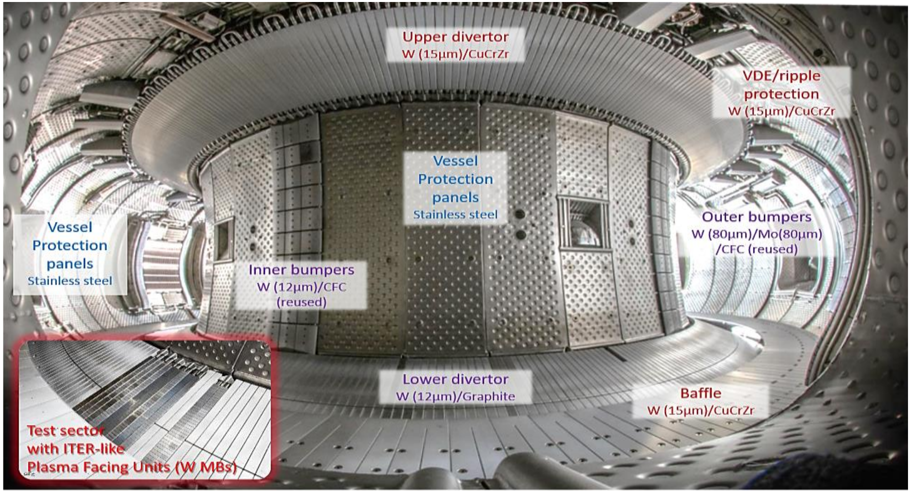

Designed for testing actively cooled ITER-like PFU

Phase I completed: with lower divertor equipped [Bucalossi NF 2022]

Phase II: plasma duration of 1000s, high performance discharges and investigation operational constraints on long durations in a W environment.

Here we will report on Phase I experiments where LHCD heating dominated.

B_T	3.7 T
R	2.5 m
a	0.4/0.5 m

Plateau Statistics Reduced L-mode Database

- The database contains the **mean values** and the **standard deviations** of different diagnostic measurements at each **plateau** (quasi-steady-state).
- The plateaus are identified intersecting the **total power plateaus** and the **plasma current plateaus**.
- There are **285** discharges with **732** plateaus in the database.

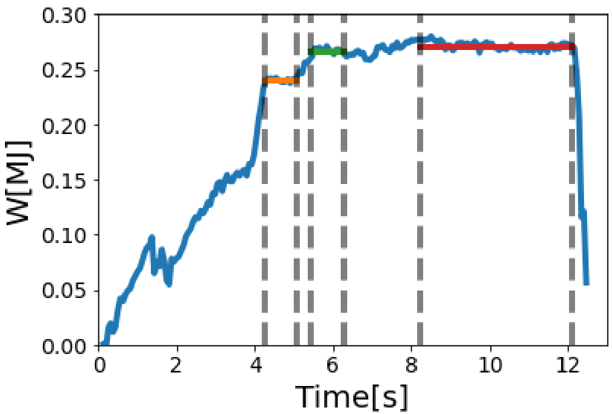

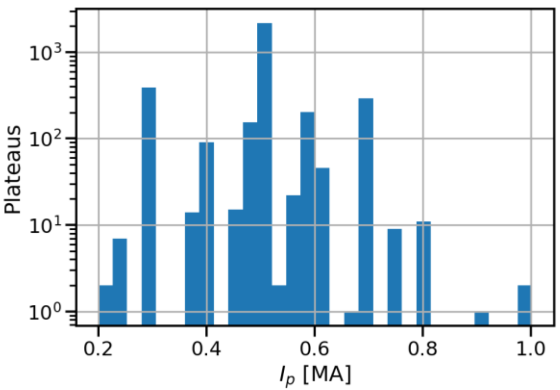

Two different confinement states coexist in WEST operation

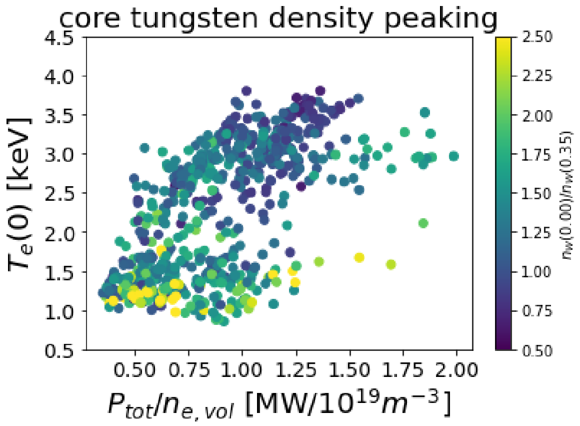

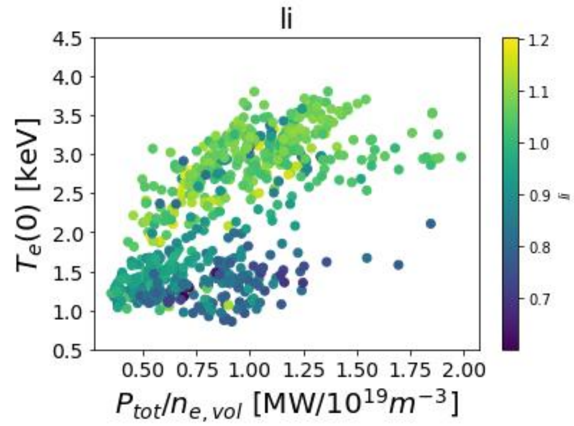

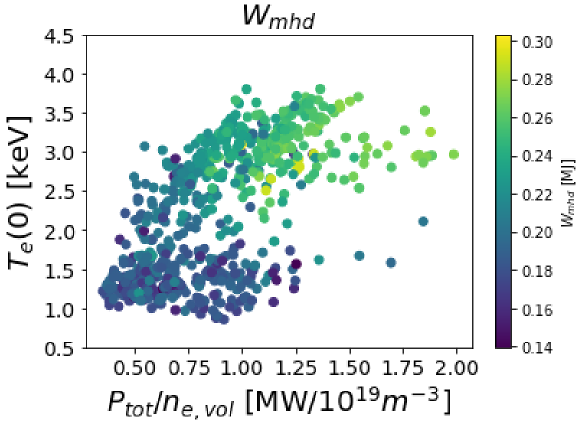

- $T_e\,(0)$ *and* W_{mhd} ↗
- *core tungsten peaking* ↘
- *li* ↗

⇓

- *less prone to mhd activity*

Central electron temperature radiative collapse

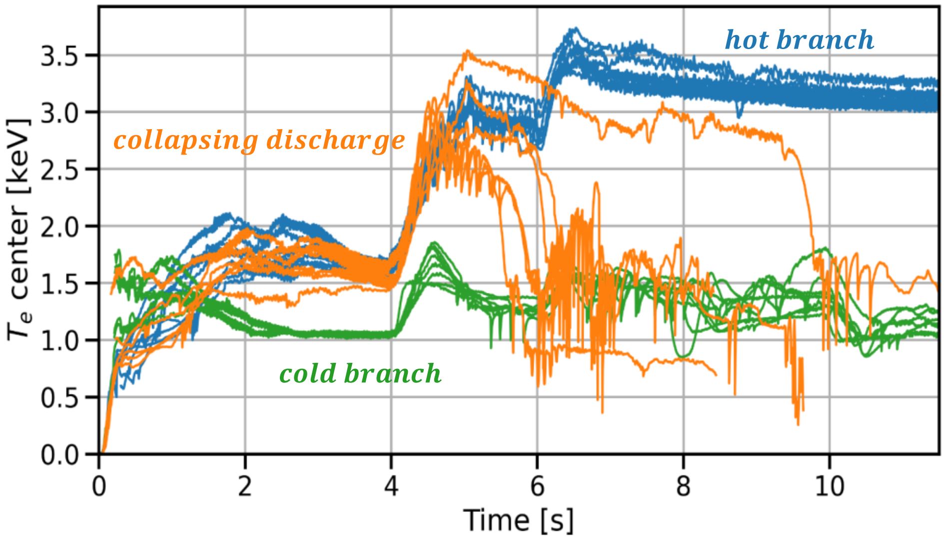

Some of the **hot branch** discharges go to the **cold branch** due to a **radiative collapse** of the central electron **temperature.**

Two questions arise from this analysis:

- Why are there two branches;
- Why the **25%** of the **discharges** in the hot branch **collapse.**

Outline

- Context;
- **Characterize and understand the dynamics of the radiative collapse observed in WEST operation;**
- Reproduce the rapid collapse of central temperature using an integrated model framework to understand which are the actuators that lead to the observed dynamics;
- Conclusions.

Characterizing the $T_e(0)$ dynamics in the database

Automatic identification of radiative collapses within plateaus:

$$exponential\ fit: \boldsymbol{T_e(0) = -e^{(a+bt)} + c}$$
$$with\ \boldsymbol{a < 0}\ for\ the\ concavity,$$

$$linear\ function\ fit$$
$$with\ \boldsymbol{slope < -830}$$

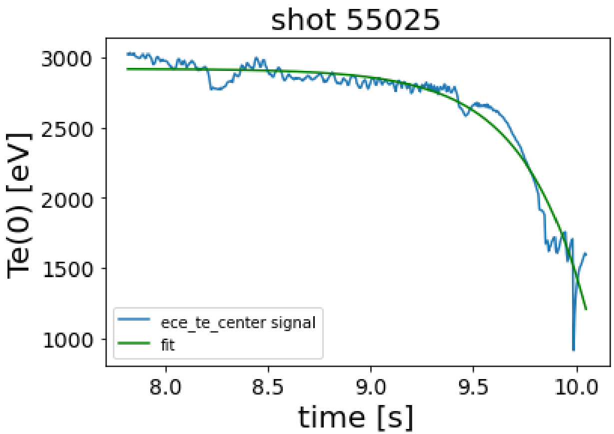

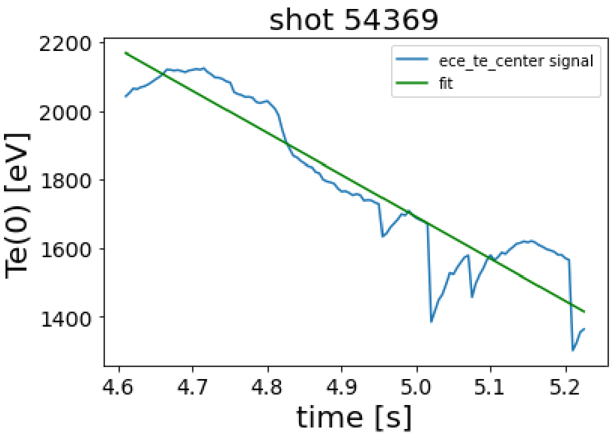

Three categories identified:
unstable plateaus where a collapse takes place, **cold stable plateaus** and remaining plateaus called **stable hot.**

Unstable plateaus consistent with W cooling factor unstable range

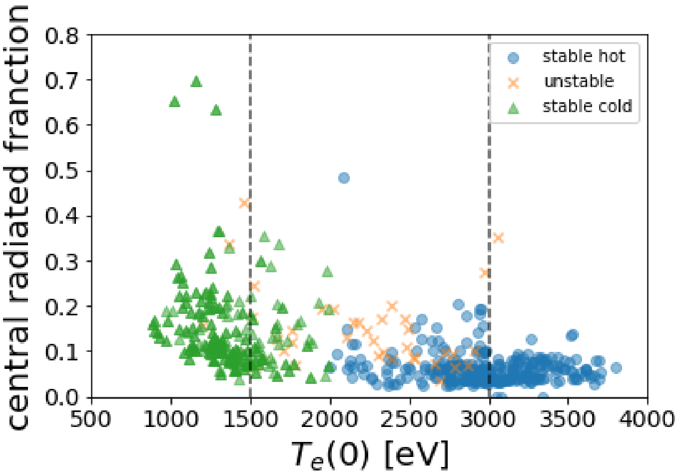

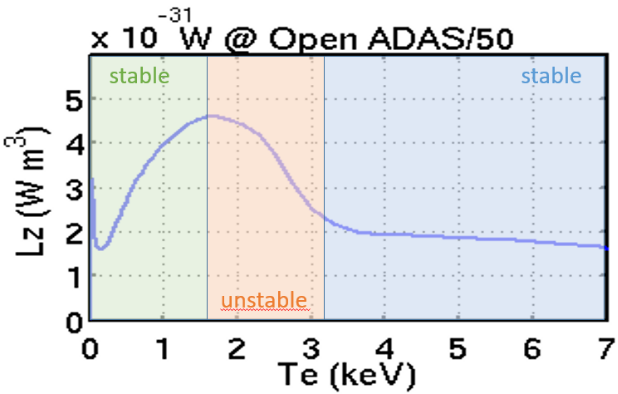

The **unstable plateaus** range between **1.5 keV** and **3 keV**. In this range, a **decrease** of electron **temperature** leads to an **increase** of **radiative losses** for the same **W content**.

25% of the **hot branch** is affected by a rapid **collapse** of the central electron temperature.

Collapsing discharge description

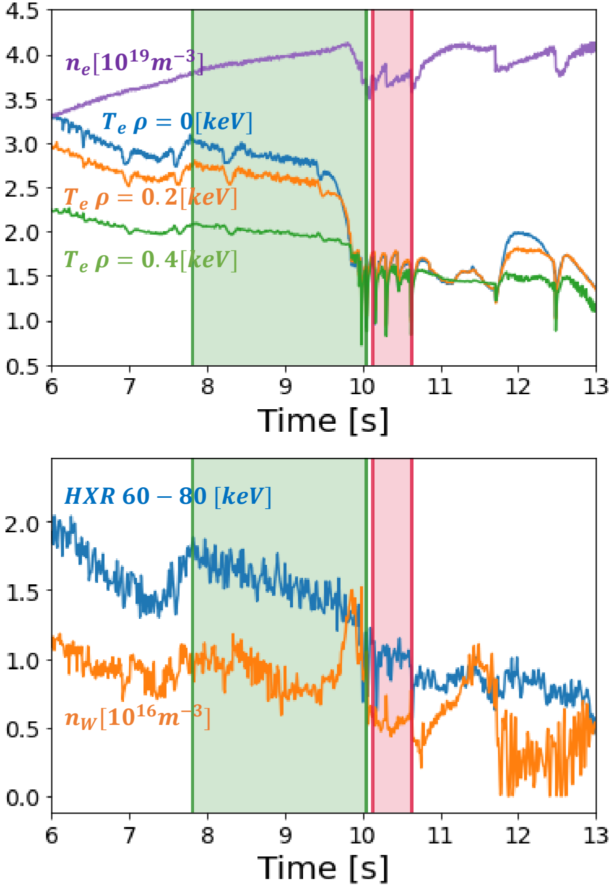

Prior to the collapse:

- a slow **increase** of **electron density;**
- a slow **decrease** of **electron temperature;**
- a **constant W** density;
- a slow **decrease** of central **HXR signal**: signature of a lower fast electron production by **LHCD.**

This complex interplay requires **integrated modelling.**

Outline

- Context;
- Characterize and understand the dynamics of the radiative collapse observed in WEST operation;
- **Reproduce the rapid collapse of central temperature using an integrated model framework to understand which are the actuators that lead to the observed dynamics;**
- Conclusions.

Integrated modelling settings

The 1D transport code **RAPTOR** is used to simulate the **collapse.** [F. Felici NF 2018]

The **transport coefficients** are computed using the **10D Neural Network version** trained on **QuaLiKiz**. [K. van de Plassche PP 2020]

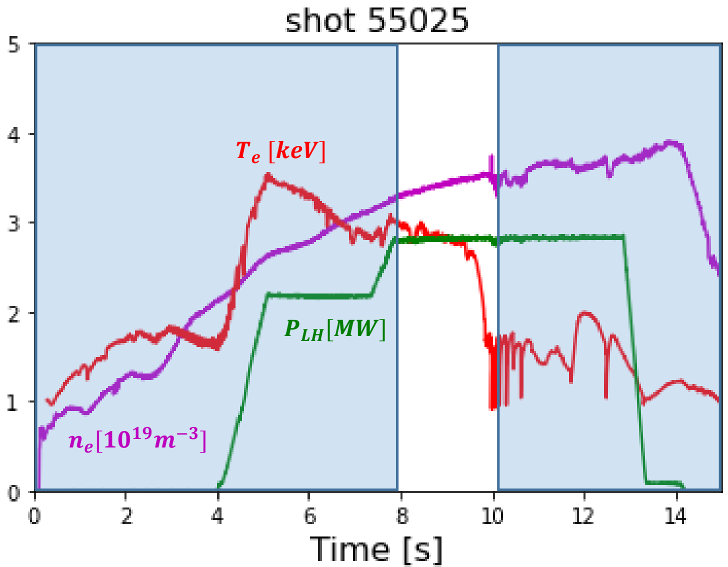

T_e and T_i	Predicted using QLKNN-10D
P_{LHCD}	LUKE [Peysson FST 2014]
n_e	interpretative
n_w	Interpretative, based on bolometry inversion
P_{rad}	Consistent with ADAS database
j(r)	predictive
equilibrium	Self-consistent inside a fixed LCFS

The $T_e(0)$ collapse is captured by the modelling

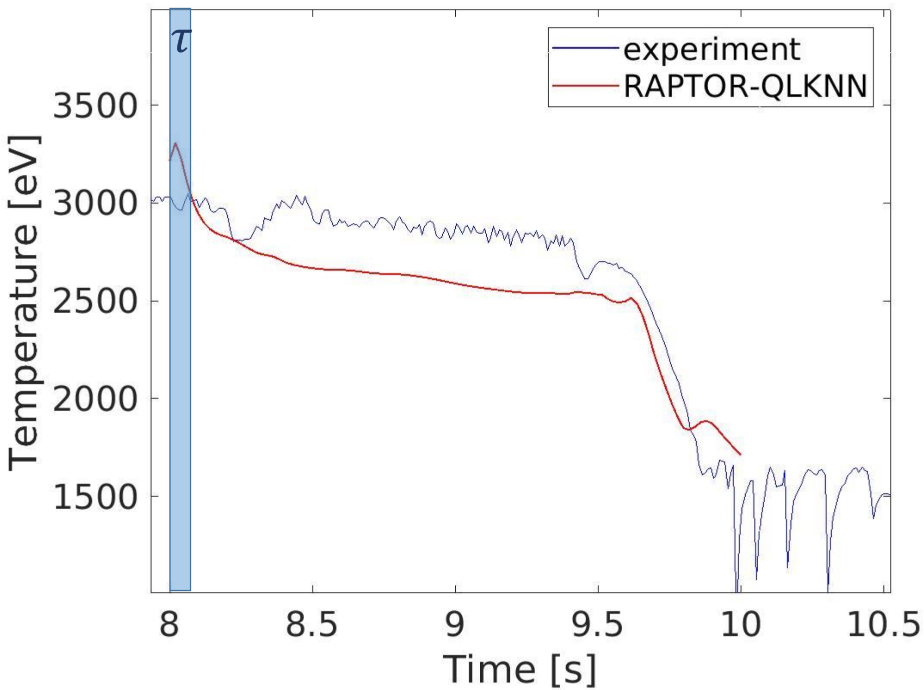

We will now investigate the role of two key ingredients: the **W profile evolution** and the **LHCD power absorption evolution.**

The T_e collapse is captured by the modelling

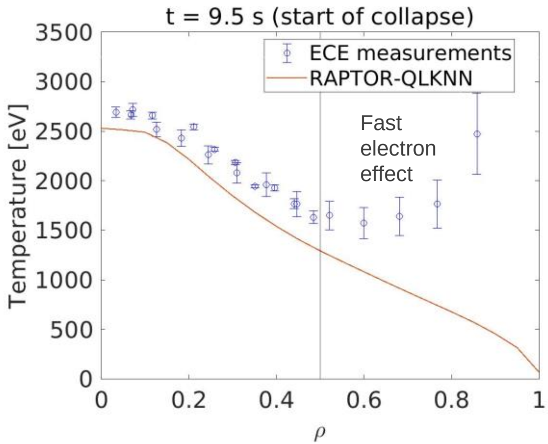

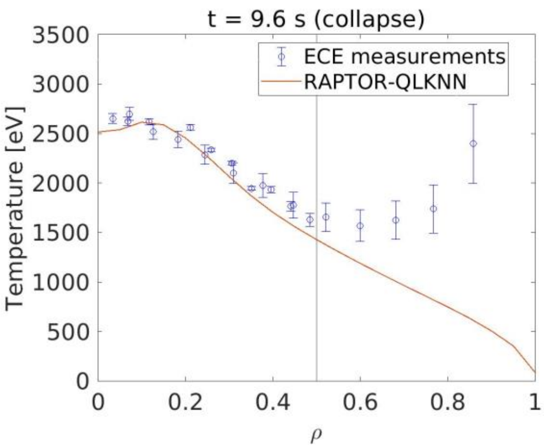

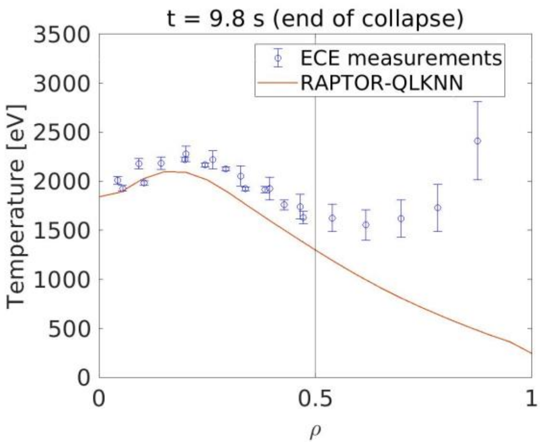

LHCD deposition is computed with the LUKE code [Peysson FST 2014]

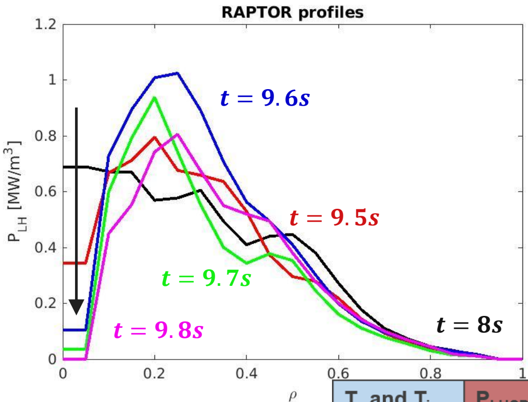

The **power deposition** in the very **core cannot be computed** with the required spatial accuracy. The **central value is adjusted** in time **to match the temperature** evolution.

A progressive **decrease** of the core electron heating by **LHCD** occurs during the slow density rise. Then it is **amplified** before the **radiative collapse**.

T_e and T_i	P_{LHCD}	n_e	n_w	P_{rad}	j(r)	equilibrium
Predicted using QLKNN-10D	LUKE	interpretative	Interpretative, based on bolometry inversion	ADAS	predictive	Self-consistent inside a fixed LCFS

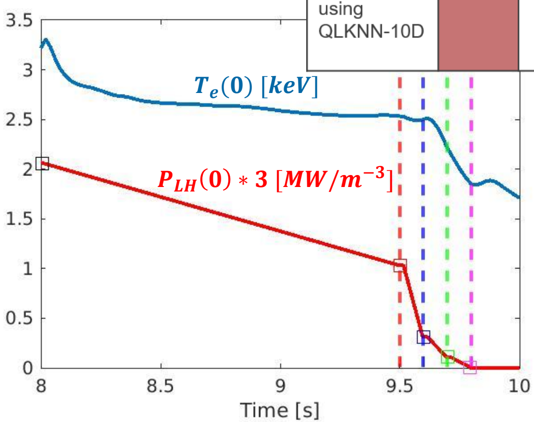

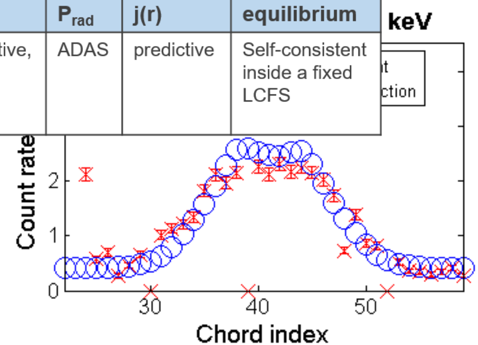

W profile obtained using bolometry measurements

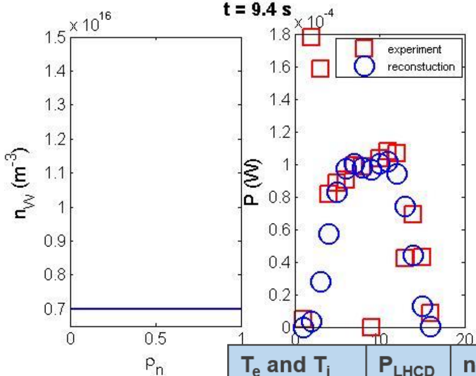

It has been assumed that n_W can be approximated by a **Gaussian symmetric** to the center of the plasma **on top of a flat profile**.
The 16 horizontal **bolomery chords** are used **to constrain the W profile** for T_e>1keV only, where the L_W are known.

T_e and T_i	P_{LHCD}	n_e	n_W	P_{rad}	j(r)	equilibrium
Predicted using QLKNN-10D	LUKE	interpretative	Interpretative, based on bolometry inversion	ADAS	predictive	Self-consistent inside a fixed LCFS

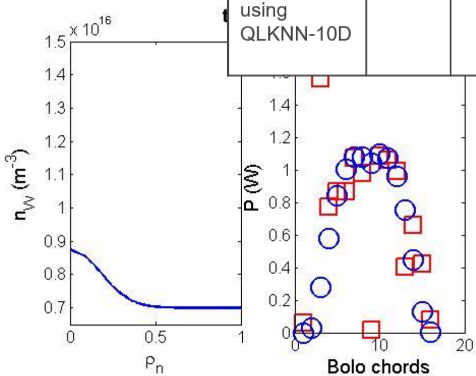

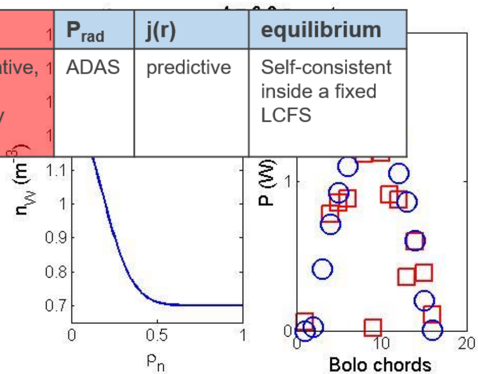

W peaking during central T_e collapse captured by reduced neoclassical T_i screening

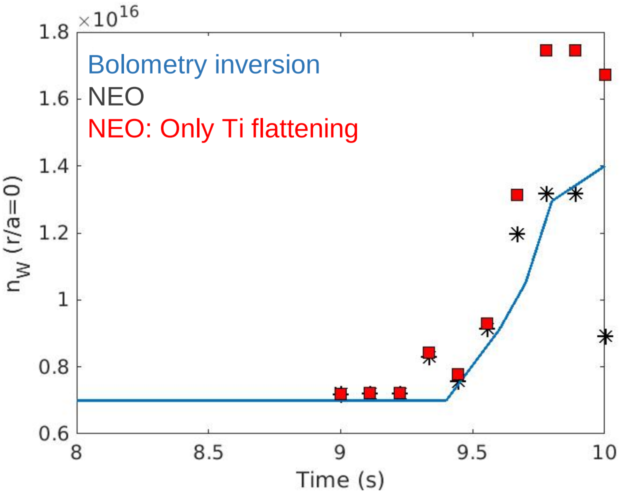

Neoclassical and turbulent transport computed with NEO [Belli 2008]

Tungsten density reconstructed from transport coefficients (BC at r/a=0.3)

In very good quantitative agreement with bolometry inferred tungsten density

W peaking increases strongly due to a core **T_e flattening**, leading to **T_i flattening** by equipartition, hence **reducing** the neoclassical **T screening effect.**

Tungsten peaking and LHCD core absorption reduction are both needed for the collapse

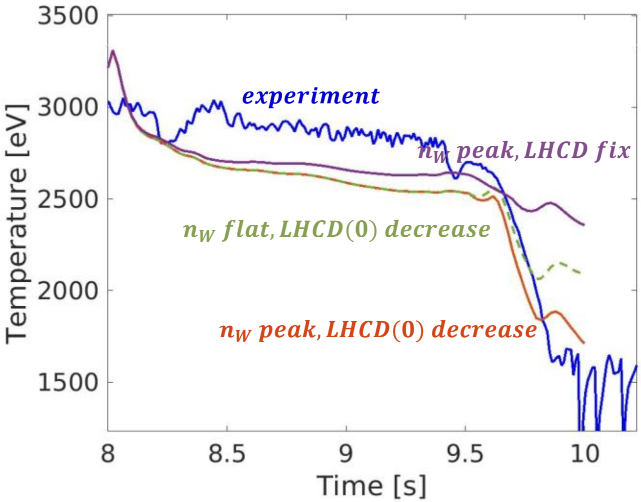

Only with both the contribution of the **tungsten accumulation** and the **decrease of** the central **LHCD** injection the **speed of collapse is reproduced.**

The **collapse** is not reproduced if the **radiated power** inside ρ=0.1 does not **overtake the central electron heating**. If core radiative fraction exceeds 1 the collapse occurs.

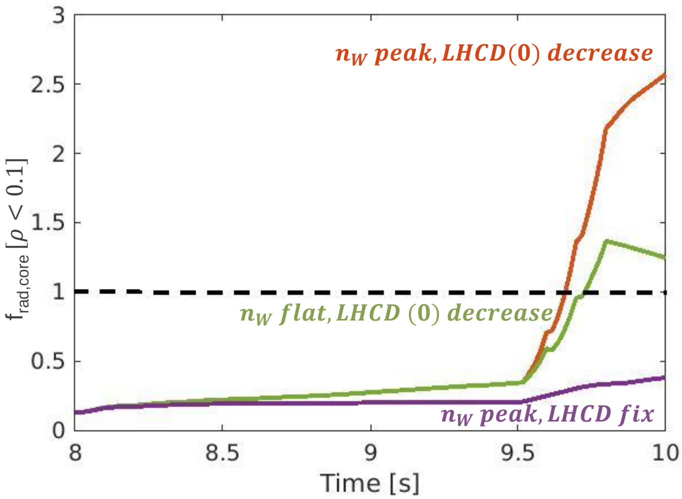

Collapse reproduction in discharge 54802

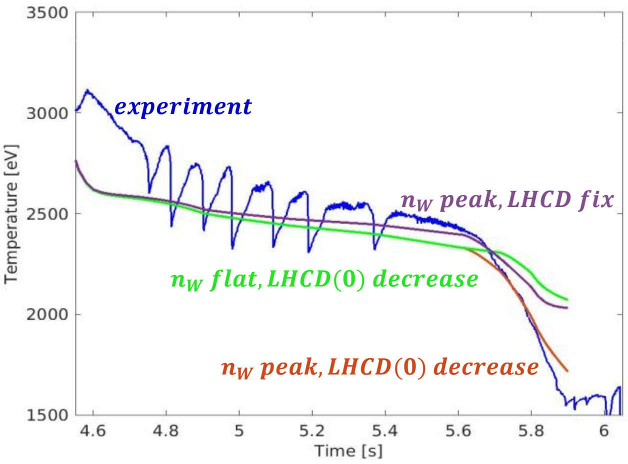

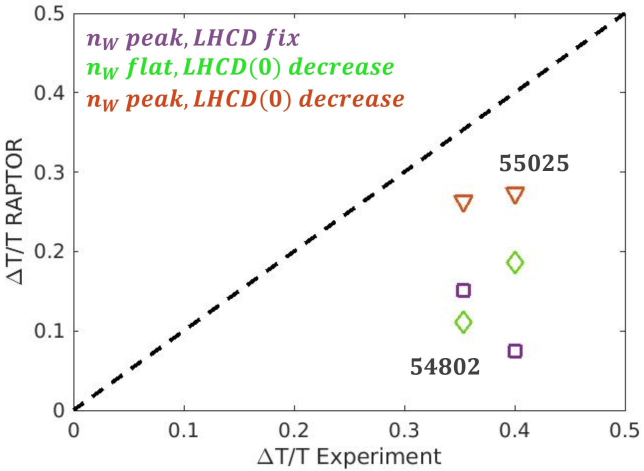

The same procedure was carried out for the **54802 discharge**.

The temperature collapses are associated to **variable contributions** of **LHCD** core heating depletion and **tungsten peaking**.

Outline

- Context;
- Characterize and understand the dynamics of the radiative collapse observed in WEST operation;
- Reproduce the rapid collapse of central temperature using an integrated model framework to understand which are the actuators that lead to the observed dynamics;
- **Conclusions.**

Conclusions

- In the database, L mode **plateaus** where $T_e(0)$ rapidly **collapse** are identified in the range of **1.5 keV** and **3 keV**.

- Time sequence of $T_e(0)$ collapse acceleration:
  - The **slight density rise** leads to **less on-axis LHCD power deposition** enhancing the central **T_e reduction**;
  - **T flattening** in core leads to a **reduction of W core temperature screening** hence **core W accumulation**

- Core **electron heating is essential** in a **W environment**.

Note: ECRH will be installed on WEST in 2023 to mitigate core LHCD deposition sensitivity

DE LA RECHERCHE À L’INDUSTRIE

BACK UP SLIDES

H_{WEST} for quantifying the quality of the confinement time

$$\tau_{mhd,measured} = \frac{W_{mhd}}{P_{tot}} = \frac{\frac{3}{2}\int_V P\,dV}{P_{ohmic} + P_{aux}}$$

$$H_{WEST} = \frac{\tau_{mhd,measured}}{\tau_{scaling}}$$

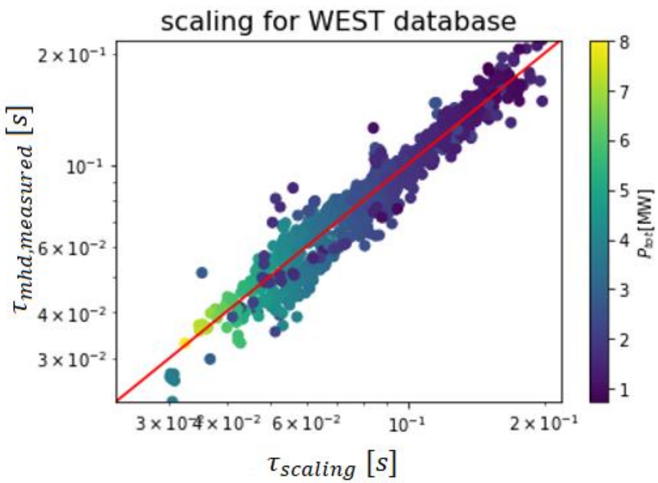

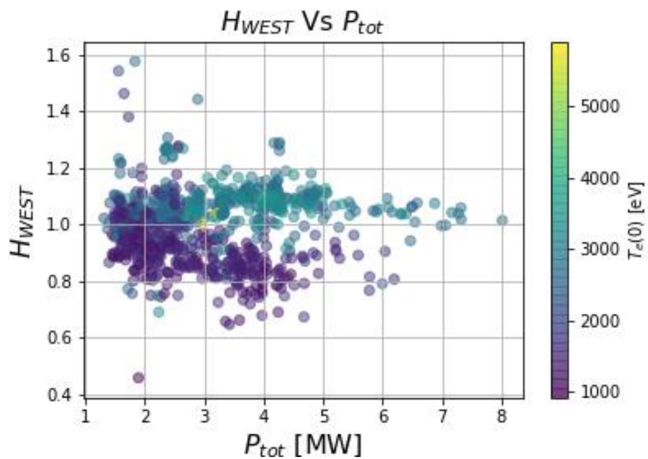

WEST database aligned with ITER96L

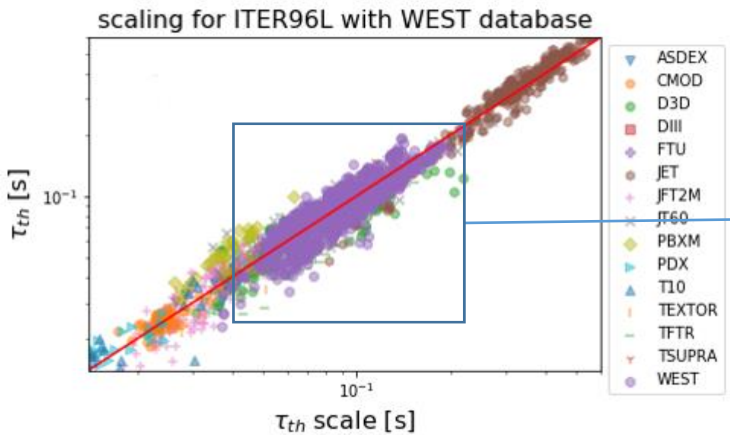

Filter:
- Small reconstruction errors;
- Diverted plasma;
- L-mode plateaus;
- LSN
- Only deuterium shots

$$\tau = C\, Ip^{\alpha_{Ip}} B^{\alpha_B} P_{tot}^{\alpha_P} n_e^{\alpha_{ne}} M^{\alpha_M} R^{\alpha_R} \varepsilon^{\alpha_\varepsilon} k^{\alpha_k}$$

$$\alpha_{Ip} = 1.35$$
$$\alpha_{n_e} = -0.16$$
$$\alpha_{P_{tot}} = -0.75$$

$$\tau_{scaling}$$

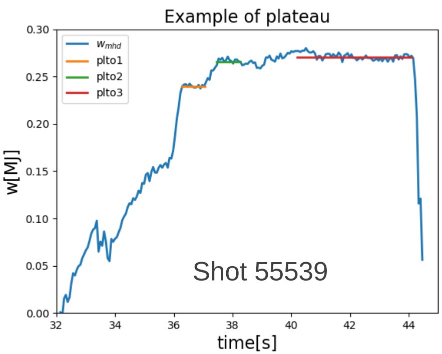

Bolometry tomography to compute the power emission density profile

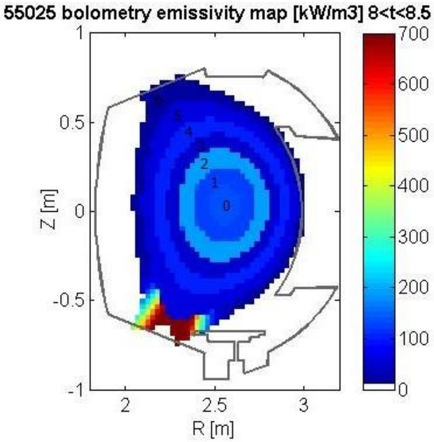

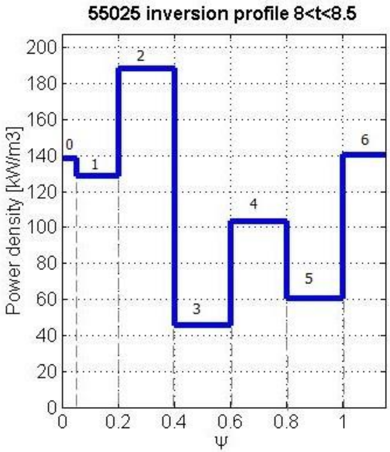

A **bolometer** measures a line-integrated value of the **local radiative emissivity** along a viewing line of sight.

A **concentric layer decomposition** of local plasma emissivity is assumed together **with asymmetric factors** in the SOL and edge. The tomography inversion is computed.

The **power emission** in $\frac{W}{m^3}$ **for each layer** are estimated.

Tungsten density profiles from the inverse of bolometry

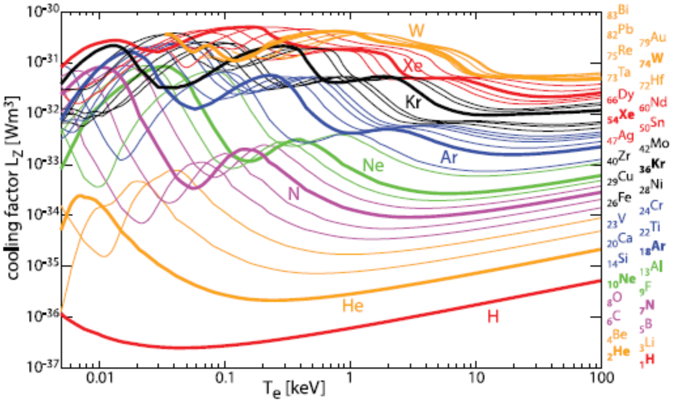

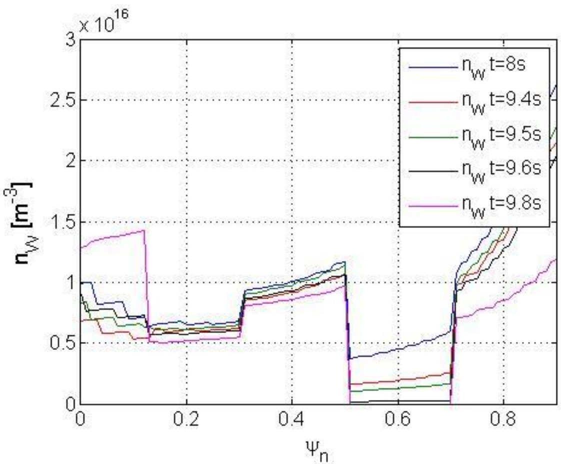

Above **1KeV** the **main radiator** is the **tungsten**.

Assuming that all the **emission radiation** comes from the **tungsten**, it is possible to use the inverse of bolometry to compute **its density** at each layer.

$$n_W \approx \frac{P_{rad,W}}{n_e L_W(T_e)}$$

$\frac{P_{tot}}{n_{e,vol}}$ for hot and cold branches and collapsing discharges

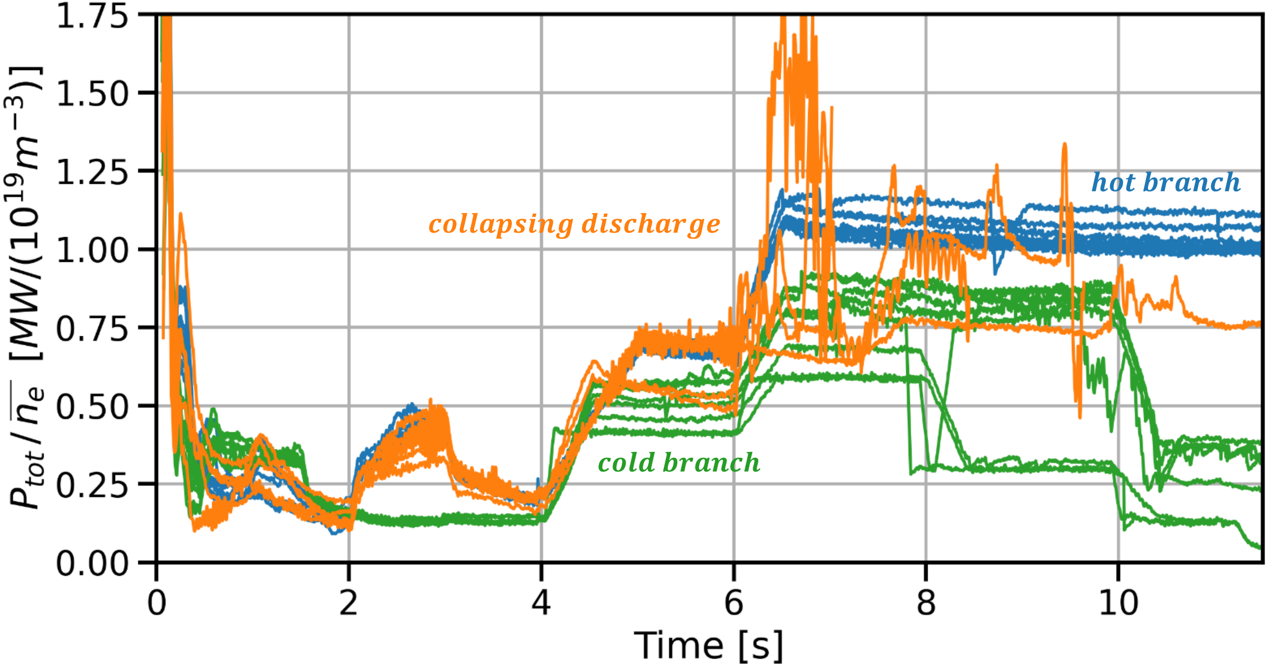

P_{LH} and $n_{e,vol}$ for hot and cold branches and collapsing discharges

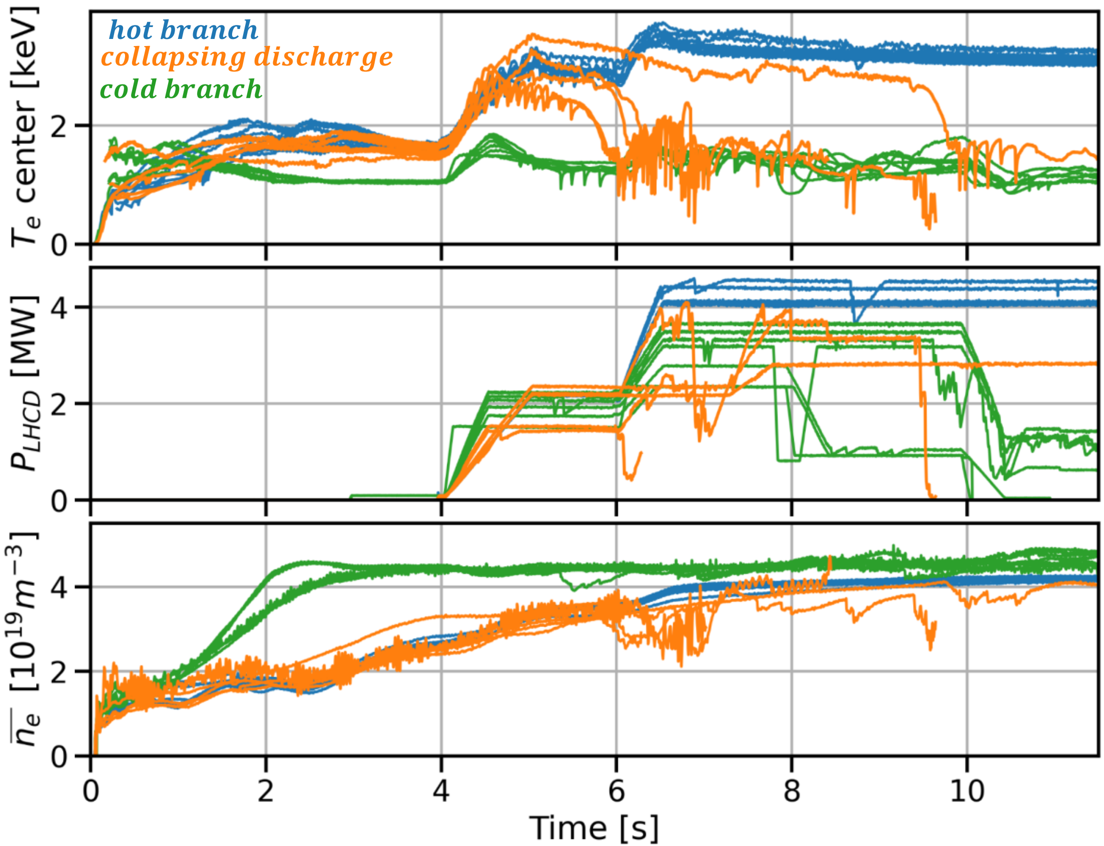

W neoclassical transport

W neoclassical transport (in absence of poloidal asymmetries)

$$\Gamma_W = -Zq^2 D n_W \left[\frac{1}{Z}\frac{\nabla n_W}{n_W} - \frac{\nabla n_i}{n_i} + \frac{1}{2}\frac{\nabla T_i}{T_i}\right]$$

Diffusion

Convection due to ion density peaking **(inward)**

Convection due to ion **thermal screening, outward**

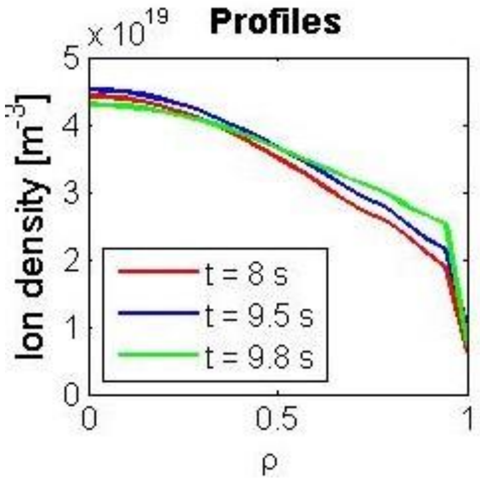

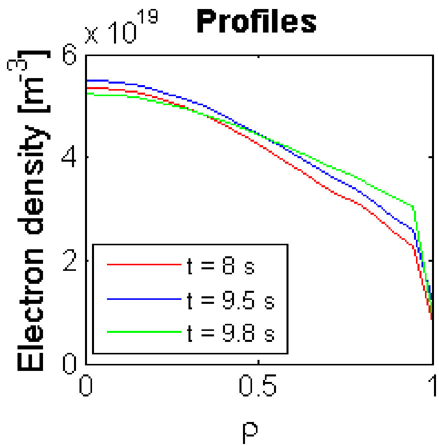

H mode

The plateaus in H mode in C4:

- In USN 4 plateaus
- In LSN 10 plateaus

Max duration of H mode on WEST 4 s.

The transitions are observed in the hot and cold branches.

The transitions are unstable because P_{rad} increases when the pedestal is formed and so the power that crosses the separator is reduced and we go back to L mode.

In C6 we will raise the density to high power because we think we were on the low density branch of the L-H transition.